Modeling of Wave Behavior of Substrate Noise Coupling for Mixed-Signal IC Design

Georgios Veronis, Yi-Chang Lu, and Robert W. Dutton
Center for Integrated Systems, Stanford University, Stanford, CA 94305
yorgos@gloworm.stanford.edu

Abstract

A new full-wave method is introduced for substrate noise analysis and simulation. The method is based on solution of the wave equation for the magnetic potential and can be implemented using standard circuit simulators. We compare the new method with the standard quasi-static method for typical substrate profiles and investigate the limits of validity of the quasi-static method.

1. Introduction

The performance of high-frequency silicon integrated circuits (ICs) is limited by parasitic coupling mechanisms in the substrate. Noise current generated by active devices is injected into and propagates through the silicon substrate. The substrate noise coupling can severely degrade the performance of sensitive circuitry [1].

Several methods have been proposed for the analysis and simulation of substrate noise [1]. Most of these methods are quasi-static (QS). In this paper, we introduce a full-wave method for substrate noise analysis. The magnetic potential (MP) method is based on solution of the wave equation for the magnetic potential.

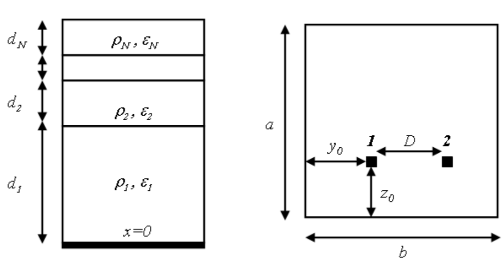

Fig. 1. Geometry of multilayer substrate.

2. Uniform lossless substrate

We first consider the simplest case of a uniform lossless substrate ($N=1, \varepsilon_1 = \varepsilon, \sigma_1 = 0$), unbounded in the y, z directions. The boundary condition at the metal ground plane (Fig. 1) is

$$\mathbf{E} \times \hat{n} = 0 \, , \, x = 0$$

The boundary condition at the upper substrate surface corresponds to zero normal electric field [2]

$$\mathbf{E} \cdot \hat{n} = 0 \, , \, x = d_1$$

Assuming no y-dependence for the fields, and using an analysis similar to that of the parallel-plate waveguide (e.g., [3]) we can show that this structure supports both *TE* and *TM* modes but no *TEM* mode. The cutoff frequency of the lowest order *TE* and *TM* modes is computed as

$$f_{c,TM_1} = f_{c,TE_1} = \frac{1}{4d_1\sqrt{\varepsilon\mu_0}} \qquad (1)$$

For a silicon substrate ($\varepsilon_r = 11.8$) the cutoff frequency calculated using (1) is approximately 54.5 GHz for $d_1 = 400\ \mu m$. In addition, at such frequencies we have $\sigma < \omega\varepsilon$ for typical high-resistivity doping profiles, so that the substrate behaves as a relatively low-loss dielectric.

Based on the above analysis, we expect that the substrate noise propagation will exhibit significant wave behavior at such frequencies at least in the case of high-resistivity substrates. The quasi-static models will be inappropriate for substrate noise analysis in these cases.

3. Formulation

3.1. Quasi-static model

We first briefly review the quasi-static formulation used in most substrate models. Starting from Maxwell's equation

$$\nabla \times \mathbf{H} = \mathbf{J} + \partial\mathbf{D}/\partial t$$

and using the identity $\nabla \cdot (\nabla \times \mathbf{a}) = 0$ and the relations $\mathbf{J} = \sigma\mathbf{E} + \mathbf{J}_s$, $\mathbf{D} = \varepsilon\mathbf{E}$, $\mathbf{E} = -\nabla\phi$ we obtain

0-7695-2093-6/04 $20.00 © 2004 IEEE
IEEE COMPUTER SOCIETY

$$\nabla\cdot(-(\sigma+j\omega\varepsilon)\nabla\phi)+\nabla\cdot\mathbf{J}_s=0$$

where $\mathbf{J}_s$ is the source current density. Integrating over a volume V and applying the divergence theorem we obtain

$$\oint_{\partial V}[-(\sigma+j\omega\varepsilon)\nabla\phi]\cdot d\mathbf{S}+\oint_{\partial V}\mathbf{J}_s\cdot d\mathbf{S}=0 \quad (2)$$

Using a finite-difference method to discretize (2) on a rectangular grid, we obtain

$$\sum_j (G_{ij}+j\omega C_{ij})(\phi_i-\phi_j)+I_{si}=0 \quad (3)$$

where the summation is taken over the 6 surfaces of the cube surrounding grid node i. I_{si} is the total source current flowing out of node i and $G_{ij}=\sigma\Delta S_{ij}/\Delta l_{ij}$, $C_{ij}=\varepsilon\Delta S_{ij}/\Delta l_{ij}$, where Δl_{ij} is the length of the grid edge connecting nodes i and j, and ΔS_{ij} is the area of the corresponding cube surface. Thus, the QS model results in a 3D mesh where each edge is a parallel combination of a resistor and a capacitor [4], as shown in Fig. 2(a).

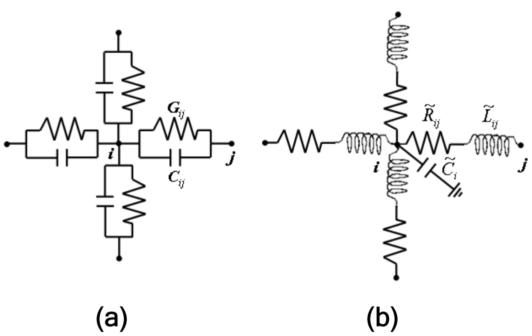

Fig. 2. (a) QS model. (b) MP model. Note that only four of the six nodes connected to node *i* are shown.

3.2. Full-wave model

We consider a uniform conducting substrate region. Using the scalar electric potential ϕ, and the vector magnetic potential $\mathbf{A}$ it can be shown [5], [6] that Maxwell's equations are equivalent to the equations

$$\nabla\cdot(-\nabla\mathbf{A})+j\omega\mu(\sigma+j\omega\varepsilon)\mathbf{A}=\mu\mathbf{J}_s \quad (4)$$

$$\nabla\cdot(-\nabla\phi)+j\omega\mu(\sigma+j\omega\varepsilon)\phi=\rho_s/\varepsilon \quad (5)$$

$$\nabla\cdot\mathbf{A}+\mu(\sigma+j\omega\varepsilon)\phi=0 \quad (6)$$

where ρ_s, $\mathbf{J}_s$ are the source charge and current densities respectively. (4) and (5) are wave equations for the magnetic and the electric potentials respectively. Equation (6) is the Lorentz condition [5]. The fields are obtained by the following equations

$$\mathbf{E}=-\nabla\phi-j\omega\mathbf{A} \quad (7)$$

$$\mathbf{B}=\nabla\times\mathbf{A} \quad (8)$$

Using the Lorentz condition (6) we obtain

$$\mathbf{E}=-j\omega\mathbf{A}+\frac{1}{\mu(\sigma+j\omega\varepsilon)}\nabla(\nabla\cdot\mathbf{A}) \quad (9)$$

We observe that in (8) and (9) the fields are expressed entirely in terms of the vector magnetic potential $\mathbf{A}$. Thus, solving (4) for $\mathbf{A}$ is sufficient to determine the fields.

Assuming that the current source $\mathbf{J}_s$ is oriented in the x-direction, and taking into account the uniformity of the region, we obtain

$$\nabla\cdot\left(\frac{-\nabla A}{\sigma+j\omega\varepsilon}\right)+j\omega\mu A=\mu\frac{\mathrm{J}_s}{\sigma+j\omega\varepsilon} \quad (10)$$

where A is the x-component of the vector magnetic potential. As in the derivation of the QS model, we integrate over a volume V and apply the divergence theorem to obtain

$$\oint_{\partial V}\frac{-\nabla A}{\sigma+j\omega\varepsilon}\cdot d\mathbf{S}+\int_V j\omega\mu A\,dV-\int_V\mu\frac{\mathrm{J}_s}{\sigma+j\omega\varepsilon}dV=0 \quad (11)$$

We use a finite-difference method to discretize (11) on a rectangular grid and obtain

$$\sum_j\frac{1}{\sigma+j\omega\varepsilon}\frac{A_i-A_j}{\Delta l_{ij}}\Delta S_{ij}+j\omega\mu A_i\Delta V_i-\frac{\mu}{\sigma+j\omega\varepsilon}\mathrm{J}_{si}\Delta V_i=0 \quad (12)$$

where the summation is taken over the 6 surfaces of the cube surrounding grid node i, and ΔV_i is the cube volume. Equation (12) can be expressed as

$$\sum_j\frac{1}{\widetilde{R}_{ij}+j\omega\widetilde{L}_{ij}}(A_i-A_j)+j\omega\widetilde{C}_iA_i+\widetilde{I}_{si}=0 \quad (13)$$

where $\widetilde{R}_{ij}=\sigma\Delta l_{ij}/\Delta S_{ij}$, $\widetilde{L}_{ij}=\varepsilon\Delta l_{ij}/\Delta S_{ij}$, $\widetilde{C}_i=\mu\Delta V_i$, and $\widetilde{I}_{si}=-\mu/(\sigma+j\omega\varepsilon)\cdot\mathrm{J}_{si}\Delta V_i$. We observe that (13) mathematically corresponds to Kirchoff's current law for a 3D mesh where each edge is

0-7695-2093-6/04 $20.00 © 2004 IEEE

IEEE COMPUTER SOCIETY

a series combination of a 'resistor' and an 'inductor'. In addition, a 'capacitor' is connected between each mesh node and the ground. Thus, the full-wave model results in a distributed RLC equivalent circuit, as shown in Fig. 2(b), where 'voltage' corresponds to the magnetic potential A. We note that $\widetilde{R}_{ij}, \widetilde{L}_{ij}, \widetilde{C}_i$ do not correspond to physical resistors, inductors, capacitors and are measured in units of Siemens/m^2, Farad/m^2, and Henry-m^2 respectively. In other words, expressing (12) as in (13) is a mathematical convenience that allows us to solve the partial differential equation (10) using the equivalent MP circuit illustrated in Fig. 2(b). A different purely resistive magnetic vector-potential equivalent circuit has been introduced by Pacelli [7] for modeling of inductive parasitics between wires.

3.3. Boundary conditions

The boundary conditions at the interface of substrate layers (Fig. 1) are

$$\mathbf{E}\times\hat{n}\Big|_{x=x_i^-} = \mathbf{E}\times\hat{n}\Big|_{x=x_i^+}, \mathbf{H}\times\hat{n}\Big|_{x=x_i^-} = \mathbf{H}\times\hat{n}\Big|_{x=x_i^+}$$

Using (8), (9) we obtain

$$A\Big|_{x=x_i^-} = A\Big|_{x=x_i^+}, \frac{\partial A/\partial x}{\sigma + j\omega\varepsilon}\Bigg|_{x=x_i^-} = \frac{\partial A/\partial x}{\sigma + j\omega\varepsilon}\Bigg|_{x=x_i^+} \qquad (14)$$

It can be shown that (14) can be incorporated into the MP circuit formulation if mesh edges at the interface between substrate layers are a parallel combination of two RL series combinations, where $\widetilde{R}_{ij}^{\pm}, \widetilde{L}_{ij}^{\pm}$ are determined by $\sigma^{\pm}, \varepsilon^{\pm}$ respectively. In addition, we have $\sigma \to \infty$ for a metal so that the boundary condition at the metal ground plane is obtained as

$$\partial A/\partial x\Big|_{x=0} = 0$$

Finally, the boundary condition at the upper surface and sidewalls of the substrate is

$$\mathbf{E}\cdot\hat{n} = 0$$

It can be shown that the corresponding boundary conditions for A are

$$\nabla A\cdot\hat{n} = 0$$

at the substrate sidewalls and

$$A\Big|_{x=x_N} = 0$$

at the upper surface of the substrate. We note that for an x-oriented current the x-component of **A** suffices to satisfy the boundary conditions.

3.4. Coupling to lumped circuits

The MP model can be coupled to lumped circuit models. We assume that a lumped x-oriented one-port circuit is connected 'in parallel' to one of the edges of the 3D substrate mesh. The lumped circuit introduces a source current $\mathbf{J}_s = \mathbf{J}_{circuit}$ in (4), where $J_{circuit} = I_{circuit}/\Delta S$. $I_{circuit}$ is the current flowing in the lumped circuit and ΔS is determined by the grid sizes perpendicular to the direction of current flow.

Let us assume that M lumped circuits are connected to the substrate, each to one of the edges of the 3D mesh. By introducing a source current $\mathbf{J}_j$ at the edge of lumped circuit j, we can use the MP model to calculate the induced voltage at the edge of lumped circuit i. In particular, (4) is solved using the MP model. Once the magnetic vector potential **A** is obtained, (9) is used to calculate the electric field **E**, and the induced voltage is obtained as $V_i = -E\Delta l$, where Δl is the edge length. Using this method, we obtain

$$Z_{ij}(\omega) = \frac{V_i}{I_j}\Bigg|_{I_k=0,\, k\neq j} \qquad (15)$$

The lumped circuits are fed with current-controlled voltage sources with transresistance Z_{ij}. The resulting coupled circuit equations are solved with one of the standard methods.

4. Results

4.1. Comparison with the FDTD method

We note that no approximations were used in the derivation of the MP model for the substrate geometry of Fig. 1. In order to test its validity, we compare it with the FDTD method [8], which is based on solution of the full Maxwell equations. There is excellent agreement between the two methods (Fig. 3). We conclude that the MP model calculates the exact full-wave solution of Maxwell's equations for the substrate geometry with accuracy similar to that of other finite-difference electromagnetic methods.

0-7695-2093-6/04 $20.00 © 2004 IEEE

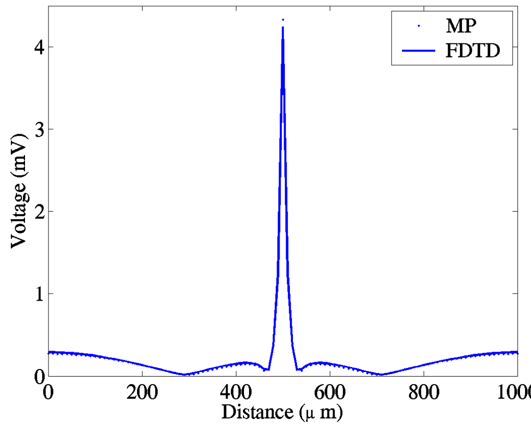

Fig. 3. Comparison between 2-D MP and FDTD methods for d_1=150 μm, d_2=140 μm, σ_1=10S/m, ε_{r1}=11.8, σ_2=0, ε_{r2}=3.9, b=1000 μm. An x-oriented current source is placed at x_s=145 μm, y_s=500 μm. We show the voltage magnitude across substrate layer *1* as a function of y.

4.2. High-resistivity substrates

We compare values of $|Z_{12}(\omega)|$ calculated by (15) for the geometry of Fig. 1 using the MP and the QS models in the case of typical substrate doping profiles [1].

Figure 4(a) shows results for a typical high-resistivity substrate profile. In agreement with the analysis of Section 2, we observe that the substrate noise propagation exhibits significant wave behavior for frequencies above approximately 20 GHz. The QS model is invalid for substrate noise analysis at these frequencies. As expected, the two models give almost identical results for frequencies up to a few GHz. In the remainder of this section, we therefore focus our attention to frequencies above 10 GHz.

In Figures 5(a), (b) we compare results for D = 200 μm, and D = 800 μm respectively. We observe that the error introduced by the QS method is smaller at smaller distances from the noise source. This is due to the fact that fields in the near zone ($D << \lambda$) are mostly quasi-static in nature [5].

In Figures 6(a), (b) we compare results for d_1 = 225 μm, and d_1 = 412.5 μm respectively. We observe that the error introduced by the QS model is large for frequencies above 90 GHz in the first case and 50 GHz in the second case. These results can be attributed to the larger cutoff frequency in the former case, as expected based on the analysis of Section 2.

In Figure 7(a) we show results for different substrate resistivities ρ_1 = 10, 50 Ω-cm. At frequencies above 50 GHz we have $\sigma << \omega\varepsilon$ in both cases, so that the substrate behaves as a relatively low-loss dielectric and induced substrate noise levels are similar. At lower frequencies, σ and $\omega\varepsilon$ are of the same order, and consequently the substrate resistivity has a significant effect (smaller resistivity results in smaller substrate noise levels).

In Figure 7(b) we investigate the effect of the low-resistivity epitaxial layer on the surface of the high-resistivity bulk region which is typical in substrate doping profiles. We observe that the thin epitaxial layer has a significant effect on the induced substrate noise levels. This is due to the fact that its resistivity is typically two orders of magnitude smaller than the resistivity of the bulk region [1].

To illustrate the coupling of the MP model with lumped circuits we simulate an example case. In Figure 8 we plot the isolation, defined as $I = 20\log(V_{out}/V_{in})$, as a function of the distance between the noise transmitter and receiver at 80GHz, calculated using the MP and QS models. As expected, at this frequency the QS model introduces significant error, particularly at large distances.

4.3. Low-resistivity substrates

Figure 4(b) shows results for a typical low-resistivity substrate profile. We observe that the error introduced by the QS model is insignificant at least for frequencies up to 100 GHz.

In low-resistivity substrates the bulk resistivity is typically four orders of magnitude lower than the resistivity of the epitaxial layer. As a result, the substrate bulk acts as a metal for frequencies up to 100 GHz. Thus, the effective length of the substrate is the epitaxial layer length d_2, typically 10 μm. Based on the analysis of Section 2, the cutoff of the lowest order propagating mode is expected to be well above 100 GHz, so that propagation is in the quasi-static regime.

0-7695-2093-6/04 $20.00 © 2004 IEEE

IEEE COMPUTER SOCIETY

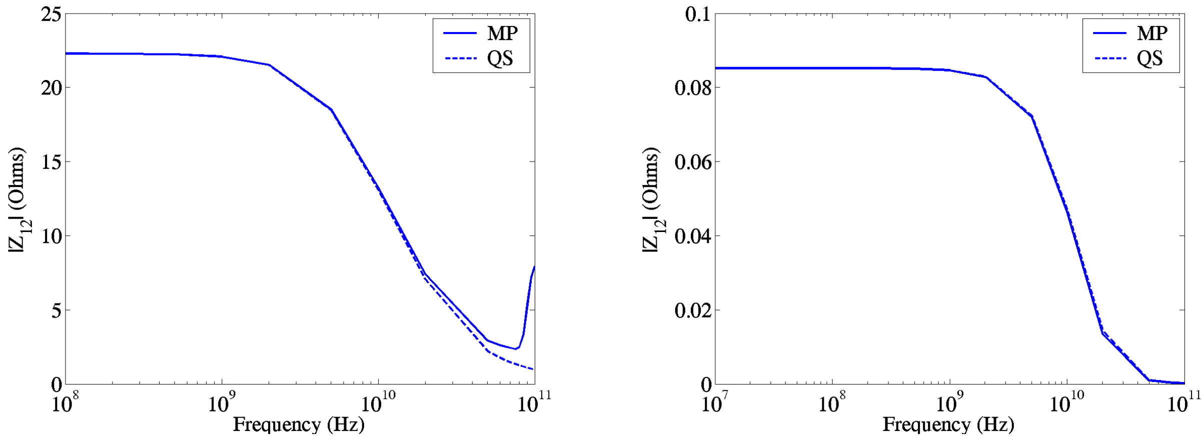

(a) (b)

Fig. 4. Simulation results. (a) High-resistivity substrate. Simulation parameters: d_1=300 μm, d_2=1 μm, ρ_1=20 Ω-cm, ρ_2=0.05 Ω-cm, ε_{r1}=ε_{r2}=11.8, a=b=1500 μm, y_0=z_0=600 μm, D=500 μm. (b) Low-resistivity substrate. Simulation parameters: d_1=300 μm, d_2=10 μm, d_3=1 μm, ρ_1=1 mΩ-cm, ρ_2=10 Ω-cm, ρ_3=1 Ω-cm, ε_{r1}=ε_{r2}=ε_{r3}=11.8, a=b=1500 μm, y_0=z_0=600 μm, D=100 μm. A uniform current density is flowing from the 25 μm X 25 μm contact to the ground.

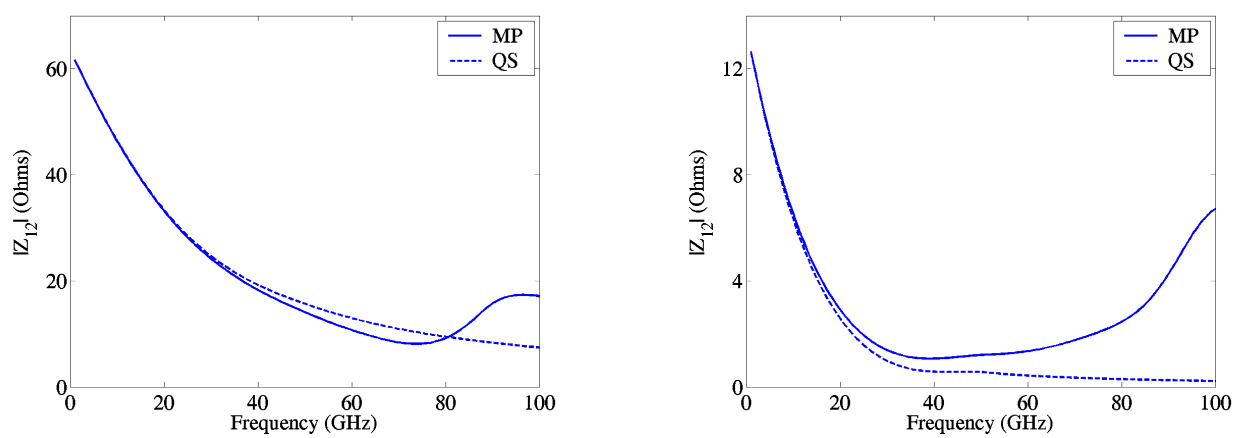

(a) (b)

Fig. 5. (a) D=200 μm. (b) D=800 μm. Other parameters are the same as in Fig. 4(a).

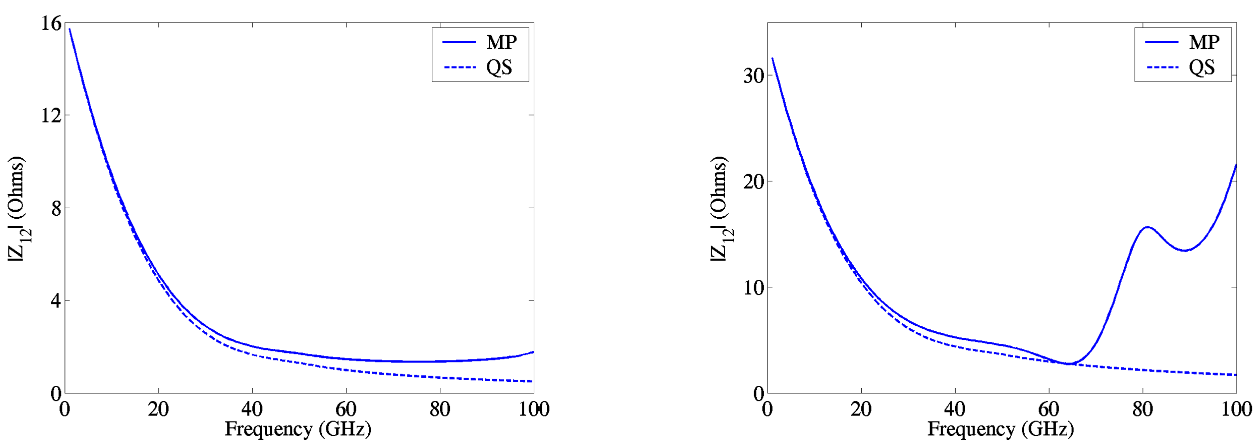

(a) (b)

Fig. 6. (a) d_1=225 μm. (b) d_1=412.5 μm. Other parameters are the same as in Fig. 4(a).

0-7695-2093-6/04 $20.00 © 2004 IEEE

IEEE COMPUTER SOCIETY

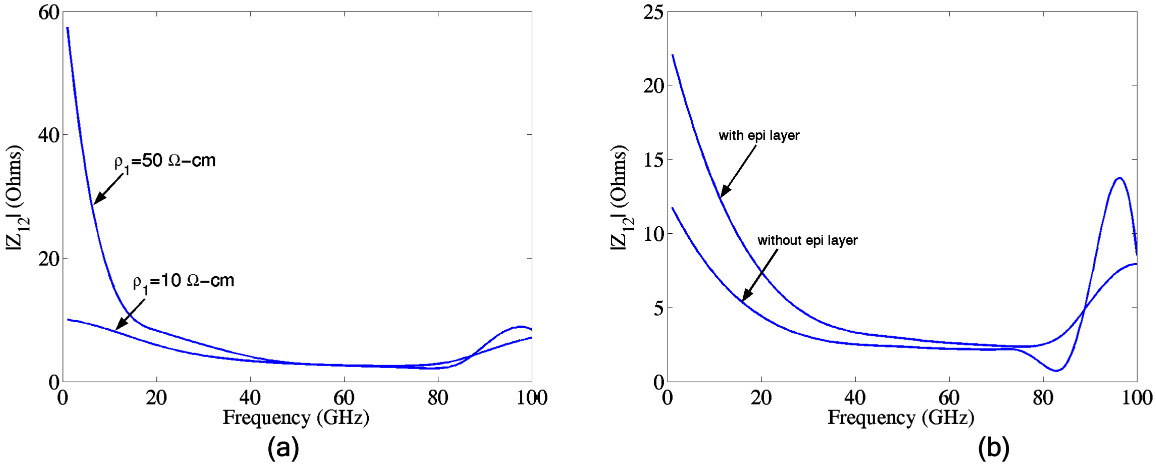

Fig. 7. (a) Effect of substrate resistivity. (b) Effect of epi layer *2*. Other parameters are the same as in Fig. 4(a). Results are calculated with the MP model.

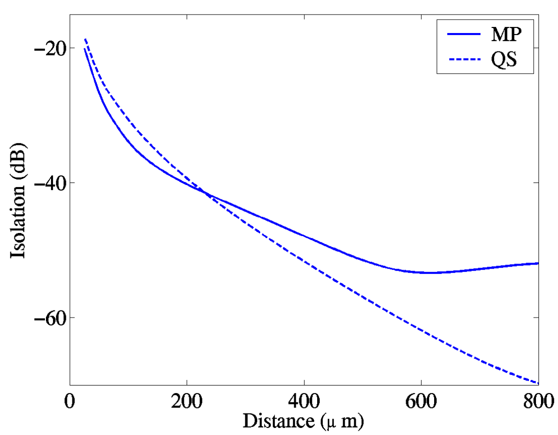

Fig. 8. Isolation as a function of *D*. Other parameters are the same as in Fig. 4(a). A voltage source V_{in} in series with a capacitor C_1=0.3pF is connected between contact *1* (Fig. 1) and the ground plane. A resistor R_{load}=50Ω in series with a capacitor C_2=0.3pF is connected between contact *2* and the ground. V_{out} is measured at the resistor.

5. Conclusions

A new fully electromagnetic method was introduced for analysis and simulation of substrate noise. The method is based on solution of the wave equation for the magnetic potential. Comparison with the FDTD method, showed excellent agreement. The new magnetic potential (MP) method and the standard quasi-static (QS) method were used to simulate both high- and low-resistivity substrates. The results showed that the QS method is invalid in the case of high-resistivity substrates at frequencies above ~20 GHz. In the case of low-resistivity substrates it is valid at least for frequencies up to 100 GHz.

6. Acknowledgements

This research was supported by DARPA under the NeoCAD project.

References

[1] E. Charbon, R. Gharpurey, P. Miliozzi, R. G. Meyer, and A. Sangiovanni-Vincentelli, *Substrate Noise, Analysis and Optimization for IC Design*, Kluwer Academic Publishers, 2001.

[2] A. M. Niknejad, R. Gharpurey, and R. G. Meyer, "Numerically stable Green function for modeling and analysis of substrate coupling in integrated circuits," *IEEE Trans. Computer-Aided Design*, Vol. 17, no. 4, pp. 305-315, April 1998.

[3] U. S. Inan, and A. S. Inan, *Engineering Electromagnetics*, Addison Wesley, 1998.

[4] B. R. Stanisic, N. K. Verghese, R. A. Rutenbar, L. R. Carley, and D. J. Allstot, "Addressing substrate coupling in mixed-mode ICs: simulation and power distribution synthesis", *IEEE J. Solid-State Circuits*, vol. 29, no. 3, pp. 226-238, Mar. 1994.

[5] J. D. Jackson, *Classical Electrodynamics*, John Wiley and Sons, 1999.

[6] J. Stratton, *Electromagnetic theory*, McGraw-Hill, 1941.

[7] A. Pacelli, "A local circuit topology for inductive parasitics", *Proc. IEEE/ACM International Conference on Computer Aided Design*, San Jose, CA, Nov. 2002, pp. 208-214.

[8] A. Taflove, *Computational Electrodynamics*, Artech House, 1995.

0-7695-2093-6/04 $20.00 © 2004 IEEE

IEEE COMPUTER SOCIETY